International Journal of Applied Engineering Research
ISSN 0973-4562 Volume 10, Number 6 (2015) pp. 14337-14349

http://www.ripublication.com

A Novel Analysis For Improvement of Power System Stability Using PSS

S.Sankar* S.Saravanakumar, D.Kamalakannan***, S.Raja*****
Professor, Dept of EEE, Panimalar Institute of Technology, Chennai Professor, Dept of IT, Panimalar Institute of Technology, Chennai,*
****Assistant Professor, Dept of CSE/IT, Panimalar Institute of Technology, Chennai*
saravanakumars81@gmail.com, ssankarphd@yahoo.com, kamal1986it@gmail.com

Abstract

The fuzzy logic system is concerned with the stability of the electric power system, and the excitation governor controllers are used to stabilize a synchronous machine infinite bus system. The considerable effort has been directed to the development power system stabilizer. Simulation results on multi machine system subjected to small perturbation and three phase fault show the effectiveness and robustness of the proposed system over a wide range of operating conditions. The problem of enhance the membership functions and the parameters of fuzzy logic based power system stabilizer is converted into an optimization problem. This paper incorporation of a simple method for the design of reliable decentralized stabilization using two controllers.

Index Terms: fuzzy logic, power system stabilizer, power system stability.

Introduction

Power systems are subjected to low frequency oscillations due to disturbances. Such oscillations may sustain and grow to cause system separation if adequate damping is not available. To enhance system damping, generators are equipped with power system stabilizers (PSSs) that provide supplementary feedback stabilizing signals in the excitation channel. Predictable PSSs are proposed in that act by adding a phase lead controller to the system. Several approaches based on modern control theory have been applied to the PSS design problem. These include optimal control, intelligent control and robust control. The majority of these applications can be found in the area of excitation control, especially power system stabilizers. In this designed power system stabilizers show promise as being less computationally burdensome and more robust than conservative power system stabilizers.

Anslysis of PSS

It contains a phase compensation network for the phase difference from the excitation controller input to the alleviate the mechanical power output. By appropriately tuning the phase and gain characteristics of this operating network, it is possible to set the desired damping ratio. In this paper a novel method is proposed to design reliable excitation and governor controllers for enhancing power system dynamic stability [1].

These are widely employed in present-day power systems to improve power system dynamic stability. It is designed for a particular operating condition around which a linearized transfer function model is obtained. The high nonlinearity, very wide operating conditions, and unpredictability of perturbations of the power system [2, 3].

A fuzzy logic power system stabilizer is basically a fuzzy logic controller [4]. According to the following are some of the major features of fuzzy logic control: model-free, in that this approach doesn't require the exact mathematical model of the system, and vigor, offering simple solutions encompassing a wide range of system parameters and significant disturbances.

The basic configuration of this system can be represented in four parts: fuzzifier, knowledge abject, inference engine and defuzzifier. “In this fuzzifier design the crisp values into fuzzy variables using normalized membership functions and input gains. The fuzzy logic inference engine then infers the proper control action based on the available fuzzy rule base [5]. In turn, the fuzzy control action is translated to the proper crisp value through the defuzzifier using normalized membership functions and system network gains.” Given the model of the FLPSS controller, we next consider the source and output to it, according to Ref. 8. For power system stabilization, speed deviation, $\Delta\omega$, and active power deviation, ΔP, or derivative of speed deviation of the synchronous machine are chosen as the FLPSS inputs.

The output control signal (U_{pss}) is the input to the automatic voltage regulator (AVR). Each of the FLPSS input and output variables, ($X_j=\{\Delta\omega,\Delta P,U_{pss}\}$), are scaled through input gains and interpreted into seven linguistic fuzzy subsets varying from Negative Big (NB) to Positive Big (PB). Each subset is associated with a triangular membership function to form a set of seven normalized and symmetrical triangular membership functions for each fuzzy variable [6,7]. A symmetrical fuzzy rule set is used to describe the stabilizer behavior. Each entity in the table represents a rule in the form “if antecedent then consequence” [8]. The objective is to design reliable decentralized excitation and governor controllers to enhance the dynamic stability of a synchronous machine infinite bus model of an operating power system, Fig. 1.

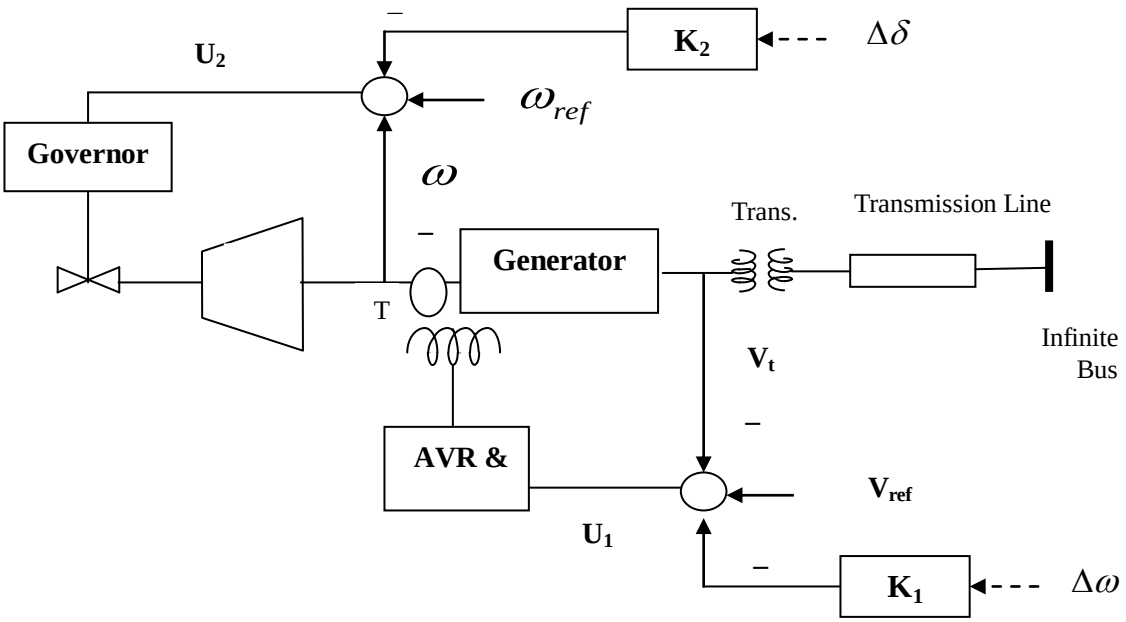

Figure 1: Schematic diagram of a single-machine infinite-bus system

The studied system is modeled as a fifth order system. A third order synchronous machine is represented by the state variable $\Delta\delta$ (incremental torque angle), $\Delta\omega$ (incremental angular velocity), $\Delta E'_q$ (incremental voltage proportional to q-axis flux linkage, under this transient reactance).In addition, a first order speed regulator is represented by the state variable ΔP_m (incremental mechanical power input), and a first order voltage regulator represented by the state variable ΔE_f (incremental field voltage) [9,10].

The dynamics of the studied system is described by

$$\begin{aligned} \dot{x} &= Ax + Bu \\ y &= Cx \end{aligned} \tag{1}$$

Where

$$\dot{x} = \begin{bmatrix} 0 & \omega_0 & 0 & 0 & 0 \\ -\frac{k_1}{M} & 0 & -\frac{k_2}{M} & 0 & \frac{1}{M} \\ -\frac{k_4}{T`_{d0}} & 0 & -\frac{1}{k_3 T`_{d0}} & \frac{1}{T`_{d0}} & 0 \\ -\frac{k_5 k_e}{T_e} & 0 & -\frac{k_6 k_e}{T_e} & -\frac{1}{T_e} & 0 \\ 0 & -\frac{1}{T_g R} & 0 & 0 & -\frac{1}{T_g} \end{bmatrix} X + \begin{bmatrix} 0 & 0 \\ 0 & 0 \\ 0 & 0 \\ \frac{k_e}{T_e} & 0 \\ 0 & \frac{1}{T_g} \end{bmatrix} \begin{bmatrix} U_1 \\ U_2 \end{bmatrix} \tag{2}$$

$$y=\begin{bmatrix}0 & 1 & 0 & 0 & 0\\ 1 & 0 & 0 & 0 & 0\end{bmatrix}x$$

Where

$$x^T(t)=[\Delta\delta \quad \Delta\omega \quad \Delta E`_q \quad \Delta E_f \quad \Delta T_m]$$

$$y^T(t)=[\Delta\omega \quad \Delta\delta]$$

and ω_0= 314

$$A = \begin{bmatrix} 0 & 314 & 0 & 0 & 0\\ -0.089 & 0 & -0.139 & 0 & 0.1\\ -0.296 & 0 & -0.463 & 0.1667 & 0\\ 131.47 & 0 & -169.62 & -20 & 0\\ 0 & -20 & 0 & 0 & -1\end{bmatrix}$$

$$B = \begin{bmatrix}0 & 0\\ 0 & 0\\ 0 & 0\\ 500 & 0\\ 0 & 1\end{bmatrix}$$

$$C = \begin{bmatrix}0 & 1 & 0 & 0 & 0\\ 1 & 0 & 0 & 0 & 0\end{bmatrix}$$

To stabilize the system in a decentralized manner, it is possible to decompose B and C as follows:

$$B = [B_1 \quad B_2], \quad C = \begin{bmatrix}C_1\\ \\ C_2\end{bmatrix}.$$

It is easy to check that the triples (C_1, AB_1) and (C_2, AB_2) are controllable and observable [11]. The transfer matrix of this system is

$$\begin{bmatrix}G_{11} & G_{12}\\ G_{21} & G_{22}\end{bmatrix} = \frac{1}{d}\begin{bmatrix}-11.57s(s+1) & 0.1s(s+2.04)(s+18.43)\\ -3634.05(s+1) & 31.4(s+18.43)(s+2.04)\end{bmatrix} \tag{3}$$

where $d=(s+18.27)(s+3.217)(s+0.971)(s^2-0.993s+30.57)$ .It is to be noticed that the open-loop system is unstable. We follow the process in the starting point of the first loop (K_1) then designing K_2 to solve the simultaneous stabilization problem, see Fig. 1.

A. Design of K_1 to stabilize G_{11}

Using the root locus technique, we design K_1 controller to stabilize G_{11} (13), The controller transfer function is selected to be

$$K_1 = -530\frac{(s^2+3.52s+12.04)}{s(s+50)}$$

The added pole at -50 is selected to be no dominant (having slight effect on the dynamic response) .This achieves a realizable proper transfer function [12]. The designed K_1 is nearly PID (Proportional Integral Derivative) control

$$K_1 = -530(3.52 + \frac{12.04}{s} + s)$$

widely used in industry.

B- Design of K_2 to stabilize G_{22} and $G`_{22}$ simultaneously

We use the relations, When K_1 fails, K_2 stabilizes the overall system if and only if it stabilizes G_{22}**.** Also, when K_1 is on, K_2 stabilizes the overall system if and only if it stabilizes G'_{22}. The transfer functions G_{22} and G'_{22} are given by

$$G_{22} = \frac{31.4(s+18.43)(s+2.04)}{(s+18.27)(s+3.2)(s+0.971)(s^2-0.993s+30.57)}$$

$$G'_{22} = \frac{31.4(s+50)(s+18.43)(s+2.04)}{(s+53.2)(s+0.985)(s^2+12.26s+57.27)(s^2+5.01s+53.66)}$$

Once again, we use the root locus technique to design K_2 that simultaneously stabilizes G_{22} and G'_{22} **.** The resulting controller transfer function is

$$K_2 = 65\frac{(s^2+0.486s+5.96)}{(s+20)^2}$$

It is to be noted that K_2 is a double lead controller.

The above controllers K_1 and K_2 achieve at least a degree of stability (0.98).

The impulse responses of the systems under reliable stabilization are shown in Figs. (2-4). As designed, the system can tolerate the outage of any of the two controllers without seriously deteriorating the degree of stability.

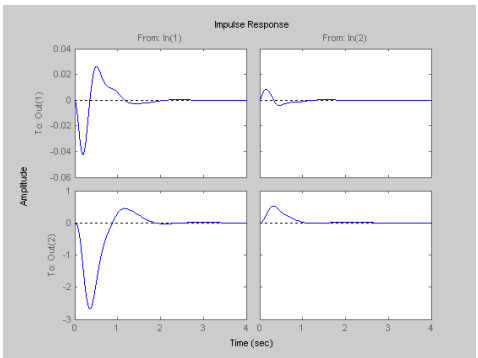

Figure 2: Impulse responses when K_1 and K_2 are active (no failure)

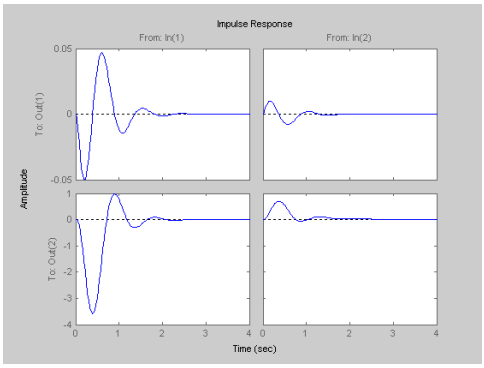

Figure 3: Impulse responses when K_1 only is active (failure in K_2)

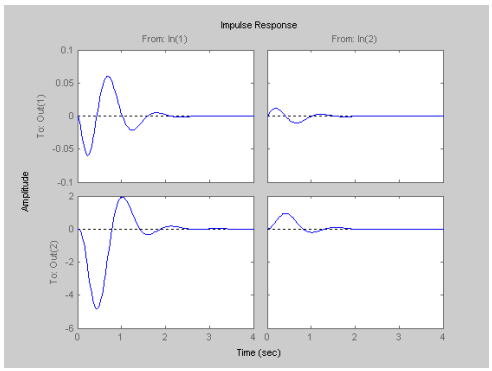

Figure 4: Impulse responses when K_2 only is active (failure in K_1).

The above analysis shows the effectiveness and robustness of the proposed reliable stabilizers and their ability to provide good damping of low frequency oscillations under different loading conditions.

Derivation of The Characteristic Coefficients

The following equations directly result from the circuit:

$$\tilde{v}_I(s)+\tilde{v}_{ac}(s)=sL_{1e}\tilde{i}_1(s) \tag{4}$$

$$\tilde{i}_1(s)=-[g_i+Y_{ac}(s)]\tilde{v}_{ac}(s)-k_i\tilde{d}_1(s)-\tilde{i}_p(s)$$

(5)

$$\tilde{i}_p(s)=-g_o\tilde{v}_{cp}(s)+k_o\tilde{d}_1(s)+g_f\tilde{v}_{ac}(s) \tag{5}$$

$$\tilde{v}_{cp}(s)=-\tilde{v}_o(s)-\tilde{v}_{ac}(s) \tag{6}$$

$$\tilde{v}_o(s)=-Z(s)\tilde{i}_p(s). \tag{7}$$

After some algebra, we can express the absorbed current at input and the injected current into the output node solely as function of the perturbations of the input voltage, duty ratio and output voltage:

$$\tilde{i}_I(s)=\tilde{i}_1(s)=\frac{K_{AI}E(s)}{N(s)}\tilde{d}_1(s)+\frac{K_{BI}(1+e_1 s)E(s)}{P(s)}\tilde{v}_O(s)+\frac{K_{CI}E'(s)}{N(s)}\tilde{v}_I(s) \quad , \tag{8}$$

$$\tilde{i}_J(s)=-\tilde{i}_p(s)=-\frac{K_{AO}F(s)}{N(s)}\tilde{d}_1(s)-\frac{K_{BO}Q(s)}{P(s)}\tilde{v}_O(s)+\frac{K_{CO}E(s)}{N(s)}\tilde{v}_I(s) \quad , \tag{9}$$

The input and output characteristic coefficients are directly identified in (8) and (9) as multipliers of $\tilde{d}_1(s)$, $\tilde{v}_O(s)$ and $\tilde{v}_I(s)$. These last equations can be written in the form

$$\tilde{i}_I(s)=A_I(s)\tilde{d}_1(s)-B_I(s)\tilde{v}_o(s)+C_I(s)\tilde{v}_I(s). \tag{10}$$

$$\tilde{i}_J(s)=A_O(s)\tilde{d}_1(s)-B_O(s)\tilde{v}_O(s)+C_O(s)\tilde{v}_I(s) \tag{11}$$

The characteristic coefficients are polynomial ratios of various degrees in variable s as it can be seen in (8) and (9).

Analysis of Open Loop Transfer Function of A System

The most general expressions of input, output and transfer properties of stabilizer such as the input and output impedance, and the input-to-output and control-to-output transfer functions can be found by means of the model with characteristic coefficients. The relationship between the output voltage and the injected current given by (11) leads to

$$\tilde{v}_O(s)=\frac{A_O(s)}{Y(s)+B_O(s)}\tilde{d}_1(s)+\frac{C_O(s)}{Y(s)+B_O(s)}\tilde{v}_I(s) \tag{12}$$

The relationship (10) contains two transfer functions of the open-loop PWM Wang converter, namely:

- the input-to-output voltage transfer function

$$H_{OI}(s)=\left.\frac{\tilde{v}_O(s)}{\tilde{v}_I(s)}\right|_{\tilde{d}_1=0};$$

- the control-to-output voltage transfer function

$$H_{OC}(s)=\left.\frac{\tilde{v}_O(s)}{\tilde{d}_1(s)}\right|_{\tilde{v}_I=0}.$$

Taking into account the expressions of the output characteristic coefficients, we found the following expressions for the transfer functions:

$$H_{OI}(s)=\frac{M(1+e_2 s)E(s)}{D(s)} \tag{13}$$

and

$$H_{OC}(s)=H_{OC}(0)\frac{(1+e_2 s)F(s)}{D(s)} \tag{14}$$

where

$D(s)=b_4 s^4+b_3 s^3+b_2 s^2+b_1 s+1$,

$H_{OC}(0)=2M(M-1)V_I/(2M-1)D_1$.

The coefficients b_k of the characteristic polynomial are functions on the effective inductances, capacities and small-signal parameters of power system stabilizer and operating point of a load.

The open-loop transfer functions of the power system stabilizer correspond to a fourth-order system, as it indicates by its diagram and (13) and (14). The expressions of the transfer functions show that their zeros are even the zeros of characteristic coefficients $A_O(s)$ and $C_O(s)$. So, if these coefficients do not contain right-half plane (RHP) zeros, neither the transfer functions do not contain them.

Using the method of time constants as explained in the numerator and denominator polynomial can be factored approximately in an analytical form. The operating conditions and circuit parameters of power system stabilizer given in the following forms:

$$E(s)=\left(1+s/Q_a\omega_a+s^2/\omega_a^2\right), \tag{15}$$

$$F(s)\cong\left(1-sf_1+s^2 f_2\right)(1-sf_3/f_2), \tag{16}$$

where $\omega_a^2=1/a_2$, $1/Q_a=a_1\omega_a$.

As it can be seen from (15), the quadratic in the numerator of the input-to-output transfer function corresponds to complex left-half-plane zeros. The factored result (16) indicates that we have three zeros of the control-to-output transfer function in the right-half plane, namely: a complex low-frequency pair well separated from a high-frequency real zero. Both transfer functions contain an extra low-frequency real zero, if $r_2\neq 0$. For the operating conditions given in the nulls of the denominator $D(s)$ can be found by other means of dealing.

The input and output small-signal properties of power system stabilizer such as the input and output impedance, can be expressed too in the terms of characteristic coefficients. Their expressions can be easily found starting from the definitions and using the corresponding small-signal equivalent circuits of converter like as in the linear

amplifier analysis. We denote with Z_g the internal impedance of line voltage source v_g. The impedance Z_{gt} includes both impedance $1/C_I$ and Z_g:

$$Z_{gt}(s)=\frac{Z_g(s)}{1+C_I(s)Z_g(s)}.$$

So, using the input-impedance definition

$$Z_I(s)=\frac{\tilde{v}_I(s)}{\tilde{i}_I(s)}$$

and the small-signal analysis of power system stabilizer is represented and the following formula of this input small-signal property results:

$$Z_I(s)=\frac{A_O(s)}{C_I(s)A_O(s)-A_I(s)C_O(s)}. \quad (17)$$

The formula (17) of the open-loop input impedance of power system stabilizer is the general expression of input impedance of switching cell in the terms of characteristic coefficients. This one is common to all the system described by means of characteristic coefficients, regardless of their topology, operating mode and control type.

After replacement of characteristic coefficients with their expressions, we found

$$Z_I(s)=\frac{K_{AO}F(s)N(s)}{K_{CI}K_{AO}E'(s)F(s)+K_{AI}K_{CO}E^2(s)}$$

(18)

Setting s at zero, the input resistance of the coupled-inductor power system stabilizer is given as $R_I=R(M-1)/M^2$. Next, we denote with Z_t the equivalent impedance

$$Z_t(s)=\frac{Z(s)}{1+B_O(s)Z(s)}.$$

Starting from the output-impedance definition

$$Z_O(s)=\left.\frac{\tilde{v}_T(s)}{\tilde{i}_T(s)}\right|_{\tilde{v}_g=0}$$

$$Z_O(s)=\frac{1}{2Y_t(s)}=\frac{R(1+e_2s)N(s)}{2[(1+e_1s)N(s)+RK_{BO}Q(s)]} \quad (19)$$

The output resistance of the coupled-inductor power system stabilizer is found as $R_O=R(M-1)/2(2M-1)$. The magnetically coupling of inductors modify the operating point of power system stabilizer with separate inductors; they are obtained by setting k_c at zero. In these conditions, $L_{1e}\to L_1$, $L_{2e}\to L_2$, $L_{em}\to L_e$ and $K_{em}\to K_e$. So, the expressions of the characteristic coefficients and small-signal properties of power system stabilizer will hold their formula and only the polynomial coefficients change the values there.

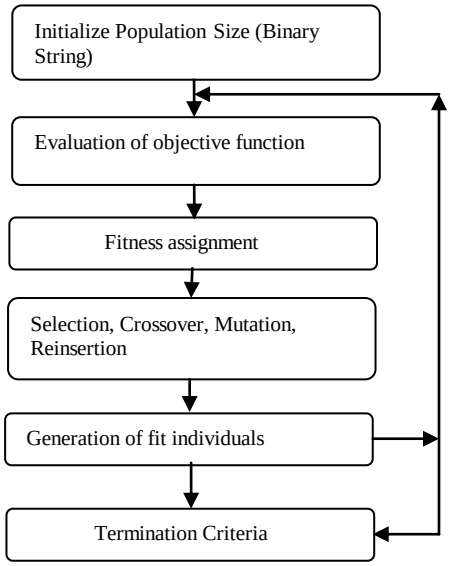

Figure 5: Flow Chart for parameter optimization using Genetic Algorithm

The ability of the system to withstand a loss of a line after a three phase fault at bus 3, for the three operating conditions is investigated by the proposed PSS. The Flow Chart for parameter is as shown in the Fig.5.

1. Operating Condition 1- Two lines between 3 and 101
2. Operating Condition 2- A single line between bus 3 and 101
3. Operating Condition 3- A single line between bus 20 and 3

A step perturbation is given and the dynamic performance of the system with the improved robust algorithm based PSS is compared with the conventional PSS and without PSS.

A. Operating Condition 1

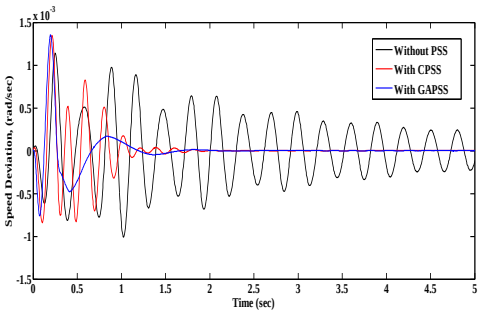

Figure 5a: Speed Deviation for operating condition 1in Generator 1

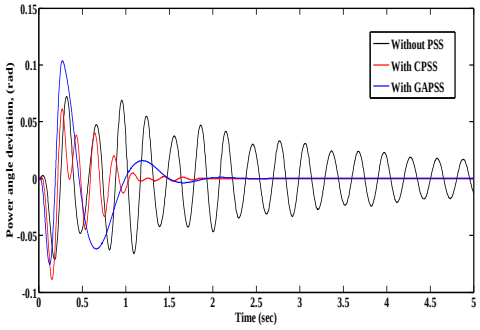

Figure 5b: Power angle deviation for operating condition 1in Generator 1

B. Operating Condition 2

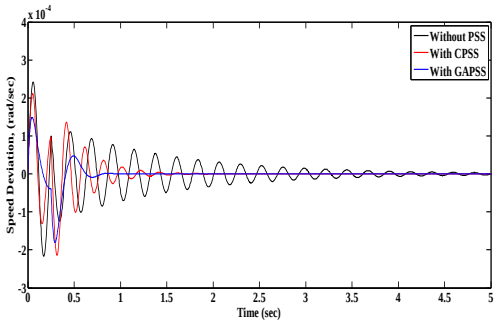

Figure 5c: Speed Deviation for operating condition 2 in Generator 11

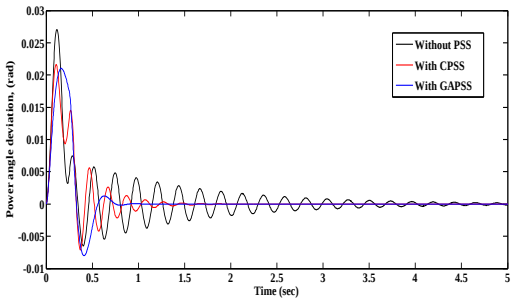

Figure 5d: Power angle deviation for operating condition 2 in Generator 11

C. Operating Condition 3

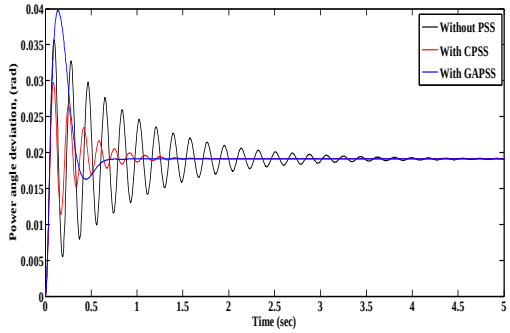

Figure 5e: Speed Deviation for operating condition 3 in Generator 12

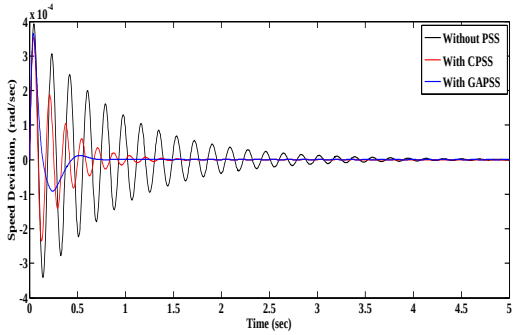

Figure 5f: Power angle deviation for operating condition 3 in Generator 12

The above simulated results show the comparison of dynamic performances under different operating conditions. Under all operating conditions only the proposed improved robust algorithm based PSS provides a very good damping (Damping time constant is between 0.5 and 2 seconds) as compared to both with conventional PSS and without PSS. Thus the new improved optimized PSS continues to perform well for all operating loads and hence has a higher level of robustness.

Conclusion

In this paper based on the efforts of fuzzy logic power system stabilizers. This algorithm is applied to a single-machine infinite-bus model. The two controllers retain the stability margin of the system when both controllers are operative and when either one of them fails. It is shown that the proposed robust optimization provides good damping characteristics and enhances the dynamic stability of the system. The simulation results of various parameter optimization techniques are analysed.This system being less computationally burdensome and more robust than conventional power system stabilizers.

References

[1]. S. Cheng, O.P. Malik, G.S. Hope, Self tuning stabilizer for a multi-machine power system, IEE Proc., Pt. 133 C (4) (2013) l76–185.

[2]. Y. Hsu, K.L. Liou, Design of self-tuning PID power system stabilizer, IEEE Trans. EC, 2 (3) (2013) 343–348.

[3]. T. Hiyama, Rule-based stabilizer for multi-machine power system, IEEE Trans. Power Syst. 5 (2) (2012) 403–411.

[4]. T. Hiyama, T. Sameshima, Fuzzy logic control scheme for on-line stabilization of multi machine power system, Fuzzy Sets Syst. 39 (2013) 181–194.

[5]. Y. Hsu, C.V. Cheng, Design of fuzzy power system stabilizers for multi machine power systems, IEE Proc. 137 (3) (2014) 233–238.

[6]. A.M. Hassan, O.P. Malik, G.S. Hope, A fuzzy logic based stabilizer for a synchronous machine, IEEE Trans. EC 6 (3) (2013) 407–413.

[7]. P. Hoang, K. Tomsovic, Design and analysis of an adaptive fuzzy power system stabilizer, IEEE Trans. EC 11 (2) (2013) 97–103.

[8]. Manisha Dubey," Design of Genetic Algorithm Based Fuzzy Logic Power System Stabilizers in Multi machine Power System", *International Conference on Soft Computing and Intelligent Systems-ICSCIS-07*, December 27-29,2010 pp 214-219.

[9]. M. A. Abido and Y. L. Abdel Magid," A Genetic-Based Power System Stabilizer", *IEEE Transactions on Electric Machines and Power Systems*, 26, 2008, pp.559-571.

[10]. Timothy. J. Ross, *Fuzzy Logic: with Engineering Applications*, Wiley, 2nd edition, 2007.

[11]. Sumathi. N, Selvan M.P, Kumaresan. N" A Hybrid Genetic Algorithm Based Power System Stabilizer", *International Conference on Intelligent and Advanced Systems* 2013, pp.876-881.

[12]. Pinaki Mazumder and Elizabeth .M. Rudnick," *Genetic Algorithms for VLSI Design, Layout and Test Automation*", Prentice Hall, 1st edition, 2013.